

Fluctuation and Noise Letters  
Vol. 2, No. 3 (2002) L183–L203  
© World Scientific Publishing Company

## PHASE LOCKING AND RESONANCES FOR STOCHASTIC EXCITABLE SYSTEMS

ANDRÉ LONGTIN

*Physics Department, University of Ottawa  
150 Louis Pasteur, Ottawa, Ont., Canada K1N 6N5  
alongtin@physics.uottawa.ca*

Received 28 June 2002

Revised 23 September 2002

Accepted 25 September 2002

We investigate the phase locking of firing events in periodically forced stochastic excitable systems. Our study is motivated by the observation of randomly phase locked firing activity in a large number of neurons, especially those involved in transducing physical stimuli such as temperature, sound, pressure and electric fields. The purpose of our paper is to review our work on the biophysical origin of such firing patterns. Special attention is given to the constructive effect of noise, and to the connection between stochastic and deterministic resonances in such systems. We present new results on stochastic phase locking in the subthreshold and suprathreshold regimes, and on the non-monotonicity of the spectral amplification as a function of noise intensity. We also discuss current outstanding problems and potentially fruitful future research directions.

*Keywords:* Neuron models; excitable system; phase locking; noise; stochastic resonance; tuning.

### 1. Introduction

The response of excitable systems to deterministic and/or stochastic forcing has received much attention in the last decades [1–4]. An excitable system is characterized by its ability to execute a large stereotyped motion in phase space when it is subjected to sufficiently strong forcing. In the case of nerve or cardiac cells, this event is usually called a “firing” or a “spike”. Such spikes propagate to other cells along axons in the case of neurons or through other kinds of electrical coupling such as gap junctions in cardiac cells. When the forcing is too weak or non-existent, the asymptotic motion of this excitable system is simply a fixed point. In the vicinity of this excitable behavior in parameter space, there usually exists a volume of parameters for which the system exhibits limit cycle behavior. In the literature, it is common to also refer to such an oscillator as an excitable system, since it can also display excitability for other parameters. Further, the phase space trajectory during the limit cycle is closely related to the stereotyped firing event. Nevertheless,

it is important to distinguish between the excitable and oscillatory regime for the purpose of understanding phase locking to periodic forcing, and in particular the effect of noise on such locking behavior.

In the excitable regime, there are different kinds of “threshold” boundaries that determine “sufficiently strong forcing” to cause a spike, depending on the nature of the bifurcation between the excitable and oscillatory regimes. If this bifurcation is of the saddle-node type, there exists a saddle point (as well as the aforementioned stable fixed point) characterized by an unstable and a stable direction (or “manifold”). The stable manifold acts as an “all-or-none” boundary for spikes: if the forcing pushes the phase space trajectory past this manifold, a spike will occur, otherwise the system relaxes back to the stable fixed point. If the bifurcation is of the Hopf-type, there is no such stable manifold, and accordingly, no true threshold. In this case, the amplitude of the phase space excursion will be a continuous function of the applied forcing magnitude; nevertheless, this function has a very steep part, with behavior similar in many respects to all-or-none behavior. The FitzHugh-Nagumo system we will focus on in this paper, as well as the Hodgkin-Huxley ionic neuron model with standard parameters, have such a graded threshold behavior.

There are two other regimes that must be distinguished within the excitable regime: subthreshold and suprathreshold forcing. The ability of a forcing signal to produce spikes is determined by its magnitude and frequency, as well as where the system lies on the line between excitable and oscillatory behavior. If the system is close to oscillatory behavior, the threshold for spiking is low, and a weak forcing signal can make the trajectory cross the threshold. If a given signal can produce spiking, it will be referred to as a suprathreshold signal; otherwise, it is subthreshold. It is important to clearly define these regimes, because they determine the main features of the response of the cell to noise and to periodic input. The frequency is also generally important because the threshold is frequency-dependent as we will see below.

Responses to suprathreshold periodic forcing include  $n:m$  phase locking patterns with  $m$  firings for  $n$  forcing cycles, as well as chaotic firing patterns [1, 4]. These patterns result from the nonlinear interaction of internal time scales of the system with the external time scale of the input. Stochastic forcing further turns a quiescent (i.e. non-firing) excitable system into a stochastic oscillator [5–7]. In other words, noise induces firing in the subthreshold regime. Alternately, when the system fires periodically (or chaotically) in the absence of noise, i.e. when the cell is in the oscillatory regime, noise turns the deterministic oscillator into a noise-perturbed oscillator. This can modify the phase locking structure, and can strongly affect the frequency sensitivity (“tuning”) characteristics of the cells [8, 10, 29]. It is also known that noise can smoothen and/or increase the dynamic range of excitable cells by linearizing their stimulus-response characteristics and breaking up phase lockings [8, 11–14]. Furthermore, other new phenomena arise from stochastic forcing, such as coherence resonance [15], stochastic resonance [3], mean frequency locking [16] and noise-enhanced phase coherence [17].

Noise in excitable systems has many possible origins, and the proportion of the different kinds of noise depends on the type of excitable cell. In the neural context (see e.g. [18]), noise arises mainly from synaptic inputs from other cells.

Noise also arises from the fluctuations in conductance of various ionic channels and ionic pumps. Some neurons, such as thermoreceptors, are free nerve endings, and their signaling of temperature does not rely on synaptic currents, but rather on the temperature-dependent rates of opening and closing of various channels [19]. Other cells that transduce physical stimuli into spikes, such as auditory and electroreceptors, involve synaptic currents at the interface between the receptor and the axon. The release rate of synaptic neurotransmitter follows the stimulus level, but there is often a strong noisy component to this rate. This results in noisy currents entering the axon, and consequently noisy firing activity. Also, certain cells such as cortical cells receive thousands of synaptic inputs which also produce stochastic firing.

This latter activity is noisy in the sense that there is a random component in the time intervals between spikes; the spikes themselves are approximately all the same once they are initiated. Thus, spike timing reflects noise in the absence of any stimuli. In the presence of stimuli, the timing of spikes depends on the signal and on the synaptic noise at the cellular level. Of course, the stimulus itself may be a stochastic process, such as band-limited Gaussian noise. Also, in the context of stochastic resonance, noise can be added to the external signal (see e.g. [20]). From a modeling perspective, one has to decide whether the internal cellular noise and external, perhaps noisy, signals can be lumped together into one term, or enter in different parts of the equations, either as multiplicative (conductance) noise or additive noise. Also, one has to consider the possibility that synaptic noise may be stimulus-dependent [21, 22].

Our paper reviews our work in the analysis of stochastic phase locking in both the subthreshold and suprathreshold regimes, and presents new results for both regimes. The subthreshold regime will be shown to be the important one from the point of view of stochastic resonance, as it is for the classic bistable potential. Further, our paper presents recent results on interesting effects of noise in the suprathreshold regime. It is our belief that this regime is very important for modeling data from certain neurons. Our focus is on dynamical models, in contrast to non-dynamical neuron models that abound in the literature (see [6], and also [23] which first analyzed a modulated shot noise process in the context of SR), and which focus solely on the statistics of the firing events without regards for how events are generated. Our paper is also meant as a brief survey of deterministic and stochastic resonances in neural systems with periodic and/or stochastic forcing. It is certainly not meant to be comprehensive, since it focusses on our own research into trying to assess the mechanisms and significance of neuronal stochastic resonance in particular, and noisy phase locked firing in excitable systems in general. We are primarily concerned with the effects of neural noise, due e.g. to ionic channel conductance, synaptic failure, and random synaptic inputs, on the encoding of time-dependent, possibly aperiodic stimuli.

Section 2 gives a brief introduction to neural models that have been studied in the stochastic neural dynamics. The FitzHugh-Nagumo (FHN) model, which will be used throughout our study, is presented there. Section 3 considers the basic response of a prototype excitable system to noise and periodic forcing of different frequencies. These basic noise, amplitude and frequency parameters will be used throughout our study to allow a comparison of the effect of these parameters on

different statistics of the spiking. Section 4 discusses the effect of noise on the deterministic resonance and tuning properties of the FHN model. We will see that noise alters the Arnold tongues of the system, and that a new kind of Arnold tongue in the noise intensity-forcing period can be used to advantage. Section 5 discusses firing statistics such as the interspike interval histogram, the spike train power spectrum and the cycle histogram for various combinations of forcing frequency and noise intensity. This sets up the results of Sec. 6 which focusses on optimal noise levels for these statistics, and their relation to the mean firing time in the presence of noise alone. Section 7 considers skipping in the suprathreshold regime, and its possible importance in modeling real neural systems. The paper concludes in Sec. 8.

## 2. Stochastic Dynamical Neuron Models

The standard dynamical description of a neuron is in terms of the Hodgkin-Huxley formalism:

$$dV/dt = \sum I_{ion} + I_{app} \quad (1)$$

$$= \sum_i g_i s_i S_i (V - V_i) + I_{app} \quad (2)$$

where  $V$  is the voltage at the spike generating zone and  $I_{app}$  designates external currents, either synaptic or from electrical (gap) coupling or from a microelectrode.  $I_{ion}$  accounts for the ionic currents, and can be divided into currents responsible for spiking and those that govern the subthreshold behavior between spikes. The  $V_i$  are the Nernst “reversal” potentials for each ionic species,  $g_i$  is the maximal conductance, and  $s_i$  and  $S_i$  are, respectively, activation and inactivation gating variables. The latter follow first-order dynamics with voltage-dependent parameters. The excitatory and inhibitory synaptic conductances may also involve gating variables and reversal potentials. Synaptic input is often modeled as a train of Dirac delta functions  $I_{syn}(t) = \sum_{i=1}^N \sum_j J_i \delta(t - t_i^j)$ , where the first sum is over all  $N$  synapses, and the second, over all firing times  $t_i^j$  at each synapse. The synaptic efficacies  $J_i$  are often lumped into one efficiency  $g$ .

An input spike train causing a sequence of synaptic currents is often assumed to be a Poisson process with rate  $N\nu$ . If  $\nu$  is large, and the  $J_i$  are small (many synaptic events must add up to fire the cell) with  $N\nu \gg 1$ , the Poisson process can be approximated by a diffusion process with same mean and variance. Thus, synaptic input may be approximated by Gaussian white additive noise on the voltage dynamics. Further, synapses also have their own first-order dynamics. Then, if the diffusion approximation is valid, the synaptic current dynamics are approximately driven by Gaussian white noise. The synaptic current is then an Ornstein-Uhlenbeck (OU) process, which in turn drives the voltage dynamics at the spike generating zone of the neuron. This justifies using OU noise for input to analytically and computationally simpler models such as the Fitzhugh-Nagumo (FHN) model [24]. This reduced model is obtained from the standard Hodgkin-Huxley model by lumping together the fast voltage and sodium activation channels together into the voltage variable  $v$ , and the sodium inactivation and potassium activation variables together

into a slow recovery variable  $w$ . In this paper, we focus on this model with additive periodic and/or stochastic forcing [24]:

$$\epsilon \frac{dv}{dt} = v(v - 0.5)(1 - v) - w + A \sin \omega_0 t + I + \eta(t), \quad (3)$$

$$\frac{dw}{dt} = v - w - b, \quad (4)$$

$$\frac{d\eta}{dt} = -\lambda\eta + \lambda\xi(t). \quad (5)$$

Here  $\xi(t)$  is Gaussian white noise of mean zero and correlation function  $\langle \xi(t)\xi(s) \rangle = 2D\delta(t-s)$ . The bias current  $I$  encompasses the mean external and synaptic currents (i.e. it is similar to  $I_{app}$  in Eq. (2)), and  $\eta$  is OU noise with variance  $D\lambda$  and correlation time  $t_c \equiv \lambda^{-1}$ . This noise is useful to investigate the effect on the dynamics of noise variance and bandwidth. Below, this system was integrated as in [25]. FHN still has realistic excitable dynamics, including a deterministic resonance. In all our simulations, a firing is counted only if separated from a previous one by at least the refractory time of  $T_R = 0.4$  sec (equivalent to  $\approx 1-2$  msec in typical real neurons). This is the time required to go along the strongly attracting excursion in phase space during the spike, and during which another spike can not be initiated no matter how large the forcing. It is important to include such a time because high noise or deterministic forcing may strongly affect the shape of the spike in model simulations, and one spike may unrealistically count as more than one if a spike is simply detected by a positive voltage threshold crossing [26].

### 3. FitzHugh-Nagumo at Different Frequencies

We wish to summarize the response properties of an excitable model to sinusoidal and stochastic forcing. We will do this in the context of the FHN model. Our work with other models suggest that the properties we will present are fairly general for neuron models. Figures 1–3 show the response to the FHN model Eq. (5) to zero-mean sinusoidal forcing and zero-mean Ornstein-Uhlenbeck noise. In all cases, the solution converges to a fixed point in the absence of periodic forcing and noise (subthreshold regime). In the presence of periodic forcing alone, the membrane voltage executes periodic motion around the fixed point (known as the “resting potential”), without spikes. In the presence of noise alone, spikes can occur, and their rate of occurrence is proportional to the noise. This is noise-induced firing (we will characterize this rate in Fig. 9 below): the noise helps the system activate over the threshold barrier.

In Figs. 1–3, firings are caused by the combination of noise and periodic forcing. It is clear that firings tend to occur near a preferred phase of the periodic forcing, but that there is randomness as well; we will refer to this form of stochastic phase locking as “skipping”. It is also clear that more firings occur as the noise intensity  $D$  increases. Figure 1 corresponds to high frequency forcing with forcing period  $T = 0.5$ ; this is a high frequency because it is on the time scale of the inverse of the refractory period. Figure 2 corresponds to a mid-range frequency (near the preferred frequency defined in the next section), and Fig. 3 to a low frequency. One can not say with confidence that spikes occur near a preferred phase of the forcing

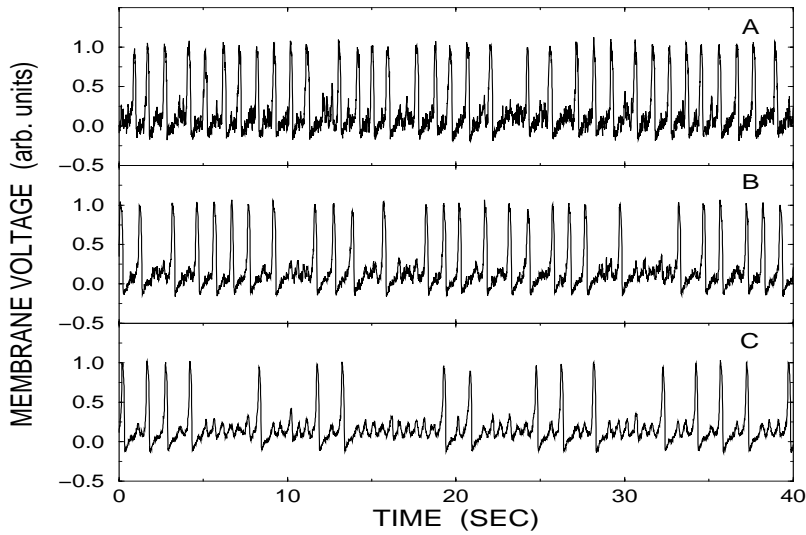


Fig. 1. Solutions of the Fitzhugh-Nagumo model Eq. (5) with high frequency sinusoidal forcing as well as broadband stochastic forcing (Ornstein-Uhlenbeck noise with correlation time  $\lambda^{-1} = 0.001$  sec). The forcing period is  $T = 0.5$  sec. The noise intensity is  $5 \times 10^{-7}$  for the lower panel,  $2 \times 10^{-6}$  for the middle panel, and  $8 \times 10^{-6}$  for the upper panel. The sinusoidal amplitude is  $A = 0.01$ , and does not produce spiking at this forcing frequency in the absence of noise, i.e. the forcing is subthreshold. Transients have been discarded. Stochastic numerical integration is done as in [25]. The time step is 0.001. Parameters are  $I = 0.04$ ,  $b = 0.15$ ,  $\epsilon = 0.005$  and are the same throughout our study unless stated otherwise.

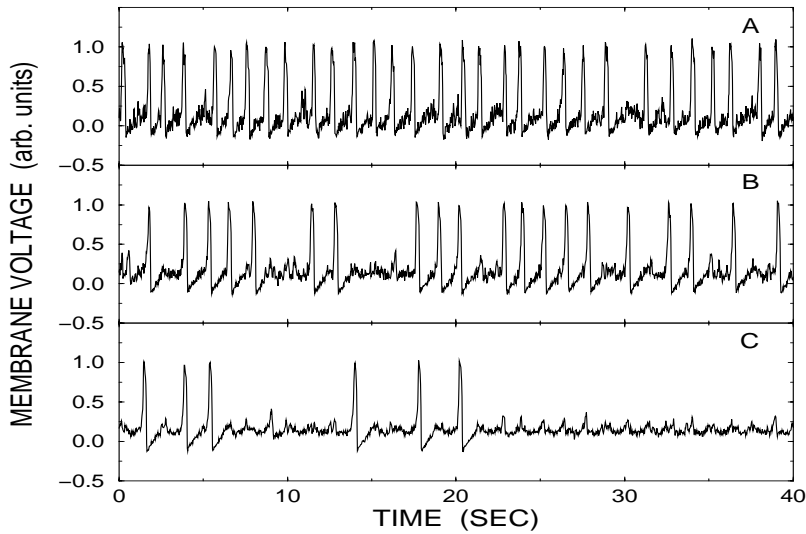


Fig. 2. Solutions of the Fitzhugh-Nagumo model Eq. (5) with moderate (“mid”) frequency sinusoidal forcing as well as broadband stochastic forcing. The forcing period is  $T = 1.25$  sec. The sinusoidal amplitude is  $A = 0.01$  (subthreshold). The noise intensity is  $5 \times 10^{-7}$  for the lower panel,  $2 \times 10^{-6}$  for the middle panel, and  $8 \times 10^{-6}$  for the upper panel. Numerical integration and parameters are as in Fig. 1.

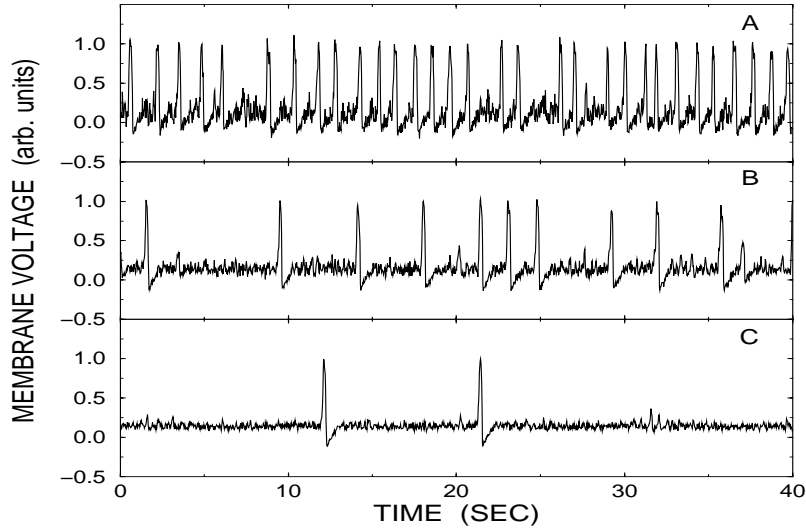


Fig. 3. Solutions of the Fitzhugh-Nagumo model Eq. (5) with low frequency sinusoidal forcing, and broadband stochastic forcing, as in Fig. 1. The forcing period is  $T = 10.0$  sec. The sinusoidal amplitude is  $A = 0.01$  (subthreshold). The noise intensity is  $5 \times 10^{-7}$  for the lower panel,  $2 \times 10^{-6}$  for the middle panel, and  $8 \times 10^{-6}$  for the upper panel. Numerical integration and parameters are as in Fig. 1.

in this last case; we will see in Fig. 6 that they do only for low noise. This is due in part to the fact that the voltage response to this low frequency forcing is small, i.e. the two-dimensional FHN model basically filters out such signals. It also filters out higher frequency signals (we return to this filtering aspect in Fig. 4).

One interesting question here is whether this model reproduces experimental data where stochastic phase locking is seen [24,27]. Other possibilities may explain a given data set, such as subthreshold chaotic dynamics [24,28]. This is a modeling question, and the usual techniques (see e.g. GlassMackey88) can be used to assess the validity and predictive power of the model. The interesting question from the point of view of stochastic resonance is: under what conditions is the periodic forcing best expressed in the output spike train, given that without noise, it is not expressed at all? The answer is, as we will see below, that a moderate amount of noise is needed if the system is in the regime used in Figs. 1–3. This in turn can help us understand how aperiodic time varying signals can be transduced by the system [26,29,30] and how the underlying deterministic resonances influence this noise-aided transduction [10,31].

## 4. Tuning and Noise

### 4.1. Preferred frequency

The FHN model has an autonomous oscillation regime arising via a Hopf bifurcation from an excitatory regime as e.g.  $I$  is increased. Consequently, it has a deterministic resonance, and behaves as an underdamped oscillator around its fixed point. This resonance may be washed out by noise, as we will see. In contrast, the

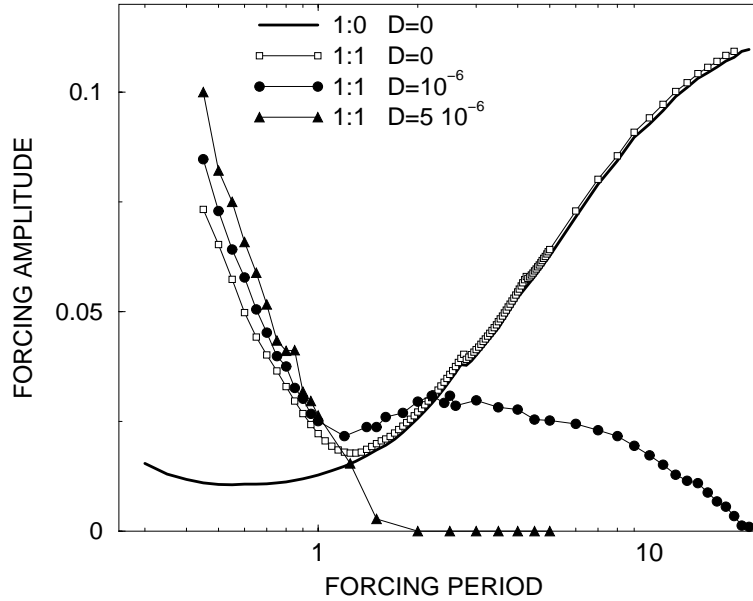
L190 *A. Longtin*

Fig. 4. Tuning curves for the Fitzhugh-Nagumo model Eq. (5) with and without noise. The noise intensity is given in the legend. In the deterministic case, each curve gives the minimum value of the forcing amplitude needed to produce one spike per forcing cycle (1:1) as a function of forcing period. In the stochastic case, each curve gives the average minimum value of the forcing amplitude needed to produce one spike per forcing cycle (1:1) *on average*, as a function of forcing period. The average minimum value is determined from three independent determinations of this minimum using parameter sweeps.

simple popular leaky integrate-and-fire model, governed by  $\dot{v} = -\alpha V + I$ , simply lowpass filters the input  $I$ . It does not have a deterministic resonance, unless one includes certain gating variables; among other things, these increase the dimensionality of the subthreshold dynamics beyond one, thereby making resonant properties possible. Figure 4 shows the organization of different steady-state periodic firing patterns in the usual signal amplitude-period subspace for the FHN model. Only two are shown for  $D = 0$ . The curves correspond to A,T pairs above which a given  $n:m$  locking occurs; these are known in the nonlinear dynamics literature as *Arnold tongue* boundaries. The subthreshold regime lies below the 1:0 curve, and the suprathreshold regime lies above this curve. One sees that the threshold for a given  $n:m$  firing depends on the forcing period  $T = 2\pi/\omega_0$ , and is lowest for its “preferred period” of  $T \approx 1.5$  sec. The preferred period for 1:1 is close to the period of the limit cycle that is reached for larger  $I_{app}$ , and to the value of  $T$  that produces the largest deterministic subthreshold voltage response (not shown). Another important observation is that the boundary between subthreshold and suprathreshold is frequency-dependent. For example, a forcing of  $A = 0.05$  is subthreshold at  $T = 10$ , but not at  $T = 1$ . Between the 1:0 and 1:1 curves one can find the classically arranged deterministic Arnold tongues [1].

It is clear that adding noise changes the shape of the curves at low to mid frequencies, but not at high frequencies. The noise can be seen as “fanning out”

the deterministic Arnold tongues into the subthreshold domain, since they are constrained (and not visible on our plot) between the 1:0 and 1:1 curves at these frequencies. The noise also blurs the boundaries between the phase locking curves. These curves can now be interpreted as A-T parameter pairs yielding a certain time-averaged phase locking ratios [10]. Thus, an  $n : 1$  ratio means an *aperiodic firing pattern* with one spike for  $n$  stimulus cycles on average. Our recent study [10] has shown that the shape of these tuning curves for  $T > 1.5$  can be deduced from an adiabatic theory based on an Arrhenius law. However, the frequency dependence of the subthreshold voltage response, related to the aforementioned deterministic resonance, must be taken into account. Without this, two forcings with same  $A$  but different  $T$  would be expected to produce the same mean firing rate, which is clearly not the case. Forcing near the resonant period of the FHN model yields large voltage responses; since these are more likely to reach threshold, spiking is then more likely to occur. For  $T < 1.5$ , the recovery variable  $w$  becomes a key determinant of the firing probability, and the whole two-dimensional escape time problem must then be studied. This has been done in the  $\epsilon \rightarrow 0$  limit in [32].

#### 4.2. $D$ - $T$ subspace and tongues

We now consider how the phase locking structure of the model looks in the  $D - T$  subspace. Figure 5 shows the location of the 1:1 “DT” Arnold tongues for two

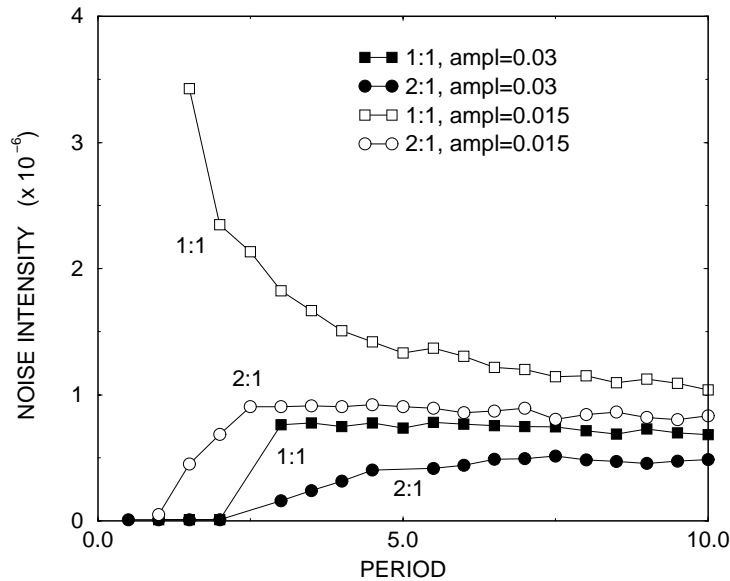


Fig. 5. Noise intensity-stimulus period boundaries for the 1:1 and 2:1 average phase locking ratios. Each curve plots, as a function of period, the minimum noise intensity needed to produce the desired average phase locking ratio. The sinusoidal forcing amplitude is set at  $A = 0.03$  for the black symbols, and  $A = 0.15$  for the open ones. Such plots can be interpreted as a new kind of Arnold tongue for stochastic excitable systems, in contrast to the usual Arnold tongues in the amplitude-period subspace of parameter space. The noise intensity simply gives an extra parameter of the forcing that can be used to characterize the phase locking properties.

different forcing amplitudes. The curves are either monotonic decreasing (1:1) or go through a maximum. It is also possible to get curves that go down, then up and then down again (from left to right), i.e. certain resonances, for parameters close to  $A = 0.015$  and 1:1 (not shown). For  $A = 0.015$ , the forcing is always subthreshold for 1:1 behavior, and noise is always needed to produce firings; a monotonic decreasing curve results. This basically means that more noise is needed to produce one spike per forcing cycle (on average) when the forcing cycle is short (i.e. the forcing frequency is high). We will see in the next section that mean 1:1 behavior occurs near the noise intensity that optimizes various statistics. However, for the other cases shown, such as 2:1, certain higher frequencies produce spikes even without noise; thus the DT tongue lies on the x-axis at those frequencies. The reason for this should be clear from Fig. 4, i.e. the threshold is frequency-dependent. As the period increases, the Arnold tongue goes up, then slowly down, interestingly exhibiting a resonance from this DT perspective.

### 5. First and Second-Order Firing Statistics

We now present a gallery of behaviors for three statistics. This is done for different combinations of noise and forcing period, keeping the amplitude fixed at the subthreshold value (for all periods) of  $A = 0.01$ . This will allow us to have a global view of the behavior of an excitable model to different regimes of stochastic and periodic forcing. The terms low, mid and high frequency are again referenced to the preferred deterministic frequency of the model (near  $T = 1.5$ , a “mid” frequency). Figure 6 shows interspike interval histograms. For the low frequency (high period)

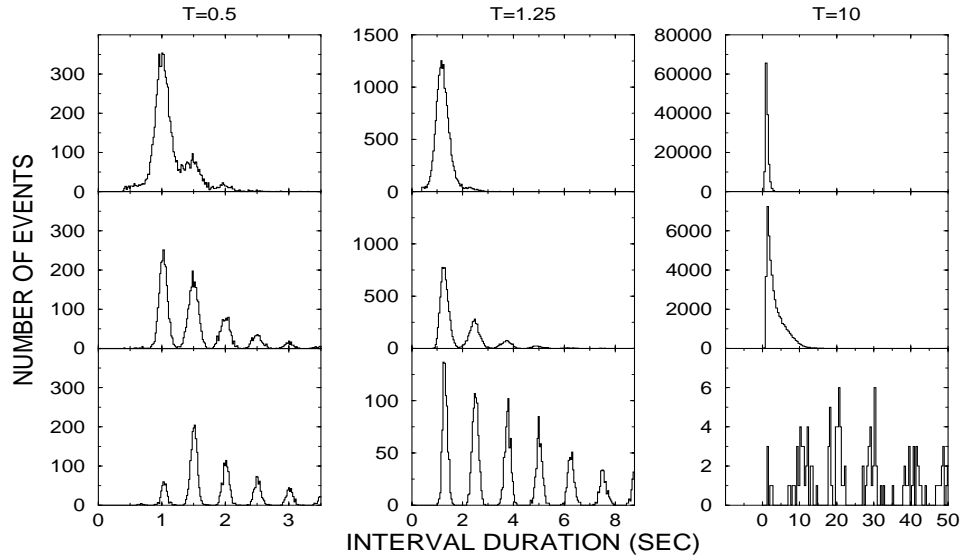


Fig. 6. Interspike interval histograms from numerical solutions of Eq. (5) for various noise intensities  $D$  and forcing periods  $T$ . The forcing amplitude is fixed at  $A = 0.01$  throughout. The ISIH's are obtained by cumulating into the same 100-bin histogram the intervals from 50 realizations of 340 forcing cycles. The noise intensity is  $5 \times 10^{-7}$  for the lower panels,  $2 \times 10^{-6}$  for the middle panels, and  $8 \times 10^{-6}$  for the upper panels.

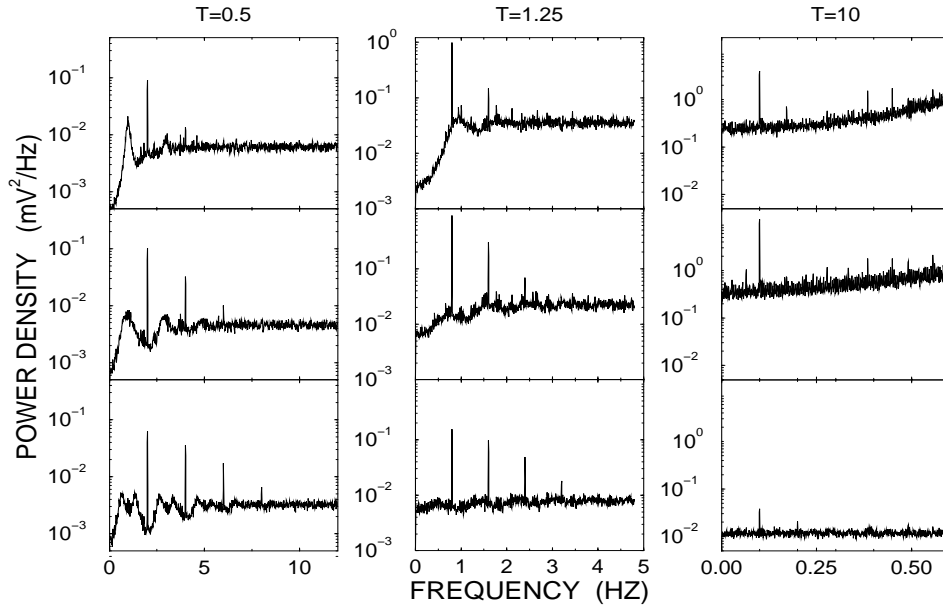


Fig. 7. Spike train power spectra from numerical solutions of Eq. (5) for various noise intensities  $D$  and forcing periods  $T$ . The forcing amplitude is fixed at  $A = 0.01$  throughout. The spectra shown are obtained by averaging the 1024-point spectra from 50 realizations of 340 forcing cycles. The spectrally flat anti-aliasing method of French-Holden was used as in [25], in conjunction with Hanning-windowing. The spectra are also averaged over the phase of the sinusoidal forcing. Noise intensities are as in Fig. 6.

$T = 10$  and low noise, a multimodal histogram is seen, as well as at mid to high frequencies and low to moderate noise levels. The qualitative similarity between 1) such experimentally observed histograms in neurophysiology and 2) those seen for bistable systems forced by noise and subthreshold sinusoids gave us the first hint that SR could be at work in excitable systems [33]. It is clear that at high noise, the histogram is unimodal, with little evidence of skipping. At low noise, there is skipping, and between the two, there is some intensity where there is a dominance of firing intervals near the forcing period. In Fig. 10, we will see that this fact reflects SR [24].

Figure 7 shows spike train power spectra for the same forcing parameter ranges. Apart from the spectral signature of the forcing signal and its harmonics, there is not much other structure for  $T = 10$ . There is more structure for lower  $T$ , relating to the presence of the refractory period; there are also modes at the mean firing rate and its harmonics. And it is clear that as noise intensity increases, the peak height at the forcing frequency  $f_0$  (also known as the spectral amplification) goes through a maximum, i.e. SR is seen (see Fig. 10).

The probability of firing as a function of the phase of the forcing signal is known as a “cycle histogram”. Such histograms are shown in Fig. 8 for the same range of parameters as Figs. 1–3 and Figs. 6–7. They have a rectified form at low noise, and become more sinusoidal at higher noise; more noise is needed for this to happen

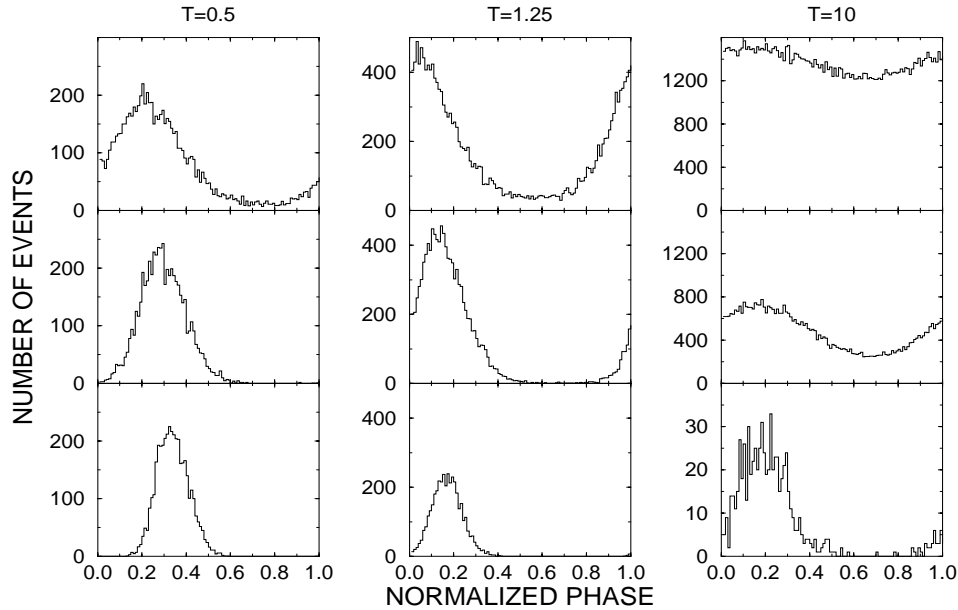
L194 *A. Longtin*


Fig. 8. Cycle histograms from solutions obtained with the same parameters as in Fig. 1. The period has been normalized to one. These histograms are constructed by incrementing one of 100 bins whenever a spike occurs at a phase of the sinusoidal stimulus corresponding to that bin. Such histograms thus represent the unnormalized firing probability as a function of stimulus phase. Results were obtained from 50 realizations of 100 cycles with  $A = 0.01$ . Noise intensities are as in Fig. 6.

when the forcing frequency is large. The transition from rectified to sinusoidal reflects the fact that the discontinuous transfer function of the deterministic neuron, which relates firing rate to bias current  $I$  in the absence of any stochastic or periodic forcing, becomes linearized by noise [26]. In fact, the slope goes through a maximum as a function of noise intensity. This linearization makes the firing probability track the forcing signal more faithfully. This can be quantified by computing the linear correlation coefficient between the cycle histogram and a sinusoid (adjusting the phase to get maximum correlation). The forcing signal will then have maximal power in the spike train near parameter values where this linearization is highest, as we will see in Fig. 11. At higher noise, the slope of the transfer function decreases again, and there is more variability in the firing events; both factors conspire to reduce the faithfulness of the rate-stimulus relation. This is the basis for SR as well as aperiodic stochastic resonance (SR for slowly varying signals [9, 26, 29]) in excitable models.

## 6. Optimal Noise

In the presence of noise and without signal, “spontaneous firing” occurs. The dependence of the mean firing rate on the noise intensity is shown in Fig. 9 for the parameters used in our study (actually the inverse of this rate is plotted). Because of the resonant nature of the FHN system, this noisy firing has a certain coherence [24].

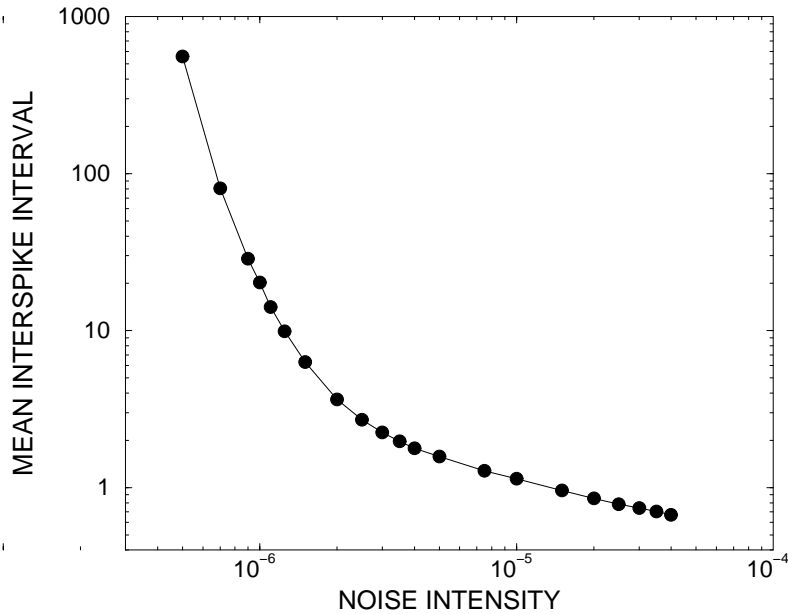


Fig. 9. (A) Mean interspike interval  $\langle ISI \rangle$  versus the noise intensity  $D$  which produces this mean firing interval for Eq. (5); there is no periodic forcing.

In fact, this coherence can be maximized by a finite noise intensity [15,32]. In other words, the noise induces the limit cycle from the excitable regime, and the regularity (“coherence”) of this limit cycle goes through a maximum at finite noise, a phenomenon referred to in this context as “coherence resonance”. This mean interval decreases as noise increases. Also, we have seen in Fig. 5 that a higher noise level is needed to obtain 1:1 firing (on average) when the mean forcing interval is small. Of course, 1:1 firing is actually a higher firing rate when the forcing period is small. From both Fig.5 and Fig.9, we can associate high noise with 1:1 at low forcing period, or with a low spontaneous firing rate. Since mean firing period and forcing are time scales, they can be plotted on the same axis.

This is done in Fig. 10, where we consider how noise maximizes various statistics introduced so far in this paper. These optimal noise ( $D_{opt}$ ) values are also calculated for a range of forcing periods. This is like doing many “SR experiments” at different forcing periods, and grouping the results all on one graph. The mean rate curve of Fig. 9 is also superimposed on the data. We see that the behavior of Fig.9 parallels the optimal noise-versus-forcing period curves for all the statistics of interest over a significant range of forcing periods [25]. For example, at higher forcing frequencies, a higher noise intensity is needed to obtain 1) 1:1 firing on average, 2) most intervals in the range of the forcing period, 3) a maximal spectral power at the forcing frequency, and 4) the best linearization. Also, at higher noise, the mean spontaneous firing interval is smaller. This is a manifestation of time scale matching of SR in excitable systems. Note also that at higher forcing periods,  $D_{opt}$  does not depend on  $T$ . This is the non-dynamical regime where the neuron acts as a simple threshold crossing

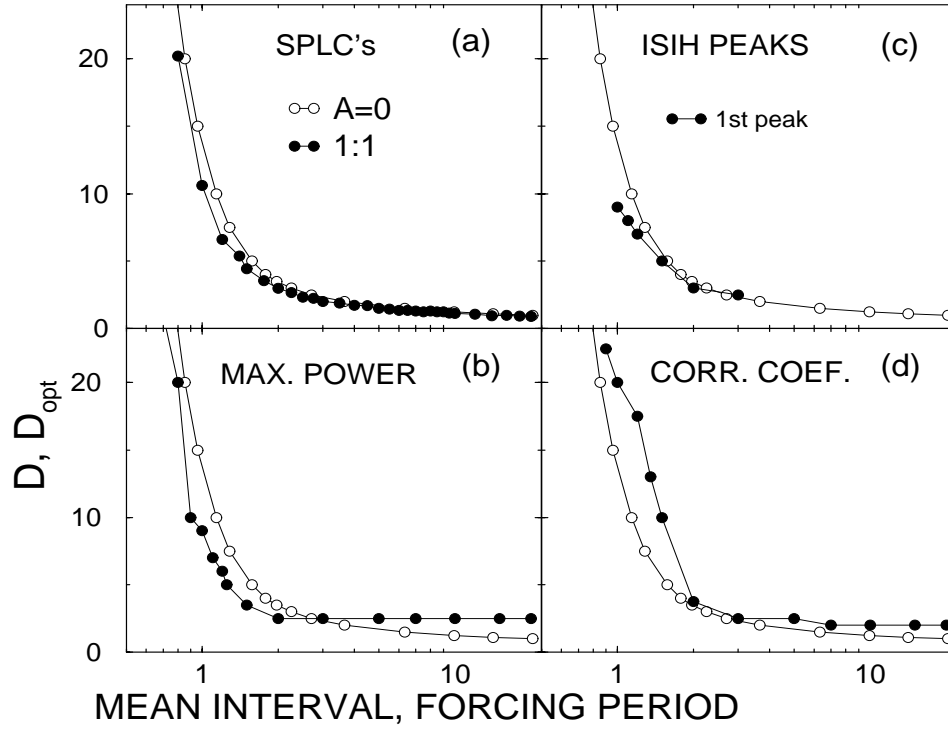
L196 *A. Longtin*


Fig. 10. Comparison of the dependence on noise of various firing statistics (filled circles and squares), and comparison of these dependencies to the mean interval curve in the absence of signal. The same (open circle) curve of mean interspike interval versus  $D$  without sinusoidal forcing,  $\langle ISI \rangle_{A=0}$ -vs- $D$  is plotted in each panel (from Fig. 9). (a) Stochastic Arnold tongue showing, as a function of  $T$ , the value  $D_{opt}$  producing on average one firing per cycle (1:1). (b)  $D_{opt}$  here yields maximal power at the forcing frequency  $1/T$  in the spike train power spectrum. (c)  $D_{opt}$  yields a maximum number of intervals of duration  $\approx T$  (first peak in the ISIH). (d)  $D_{opt}$  yields the maximum linear correlation coefficient between the sinusoidal forcing and the time-dependent firing probability. In (b), (c), (d), dynamical refractory effects occur for  $T < 3$  approximately, and statistics with signal parallel the zero-signal mean interval. A static regime occurs for  $T > 3$ , where  $D_{opt}$  is independent of  $T$ . Symbols are approximately two standard deviations wide.

device [34, 35]; this occurs clearly when the time scale of the periodic forcing is larger than all internal system time scales.

At higher frequencies, it is known that nonlinear phase locking phenomena occur in the suprathreshold regime. For subthreshold signals, we have found that multiple stochastic resonances can occur as  $D$  increases [25]. Here we show in Fig. 11 new results on the transition from a simple stochastic resonance to double stochastic resonance in the FHN system as  $T$  decreases. For  $T = 1.0$ , a single maximum is seen, while for  $T = 0.6$ , two bumps are seen. Such multiple resonances were found when  $T < 0.9$ . Similar resonances have also been found in bistable systems [36]. These subthreshold resonances are perhaps related to the deterministic lockings that exist for suprathreshold forcing, and which are induced by the noise. This is currently under investigation.

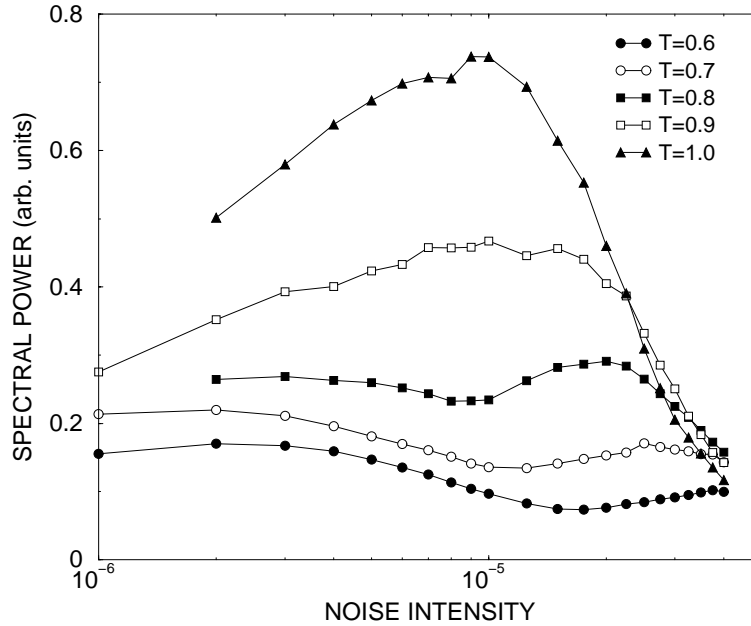


Fig. 11. Spectral power at the forcing frequency computed from spike trains, plotted as a function of noise intensity  $D$  for different forcing periods  $T$ . As the frequency increases, the curves acquire more local minima, and the maximum power occurs at lower  $D$  values.

## 7. Suprathreshold Skipping

The SR literature is rife with examples of stochastic phase locking with subthreshold periodic signals. This produces the familiar multimodal residence time histograms [3]. Suprathreshold signals can also produce such behavior in the FHN system [24]. The histogram peaks in that latter study did not perfectly align with the integer multiples of the forcing period, and the histogram envelope did not vary smoothly with forcing parameters as it did in experimental data and in the subthreshold regime. This was in contrast to what was observed experimentally in e.g. auditory cells. This was in part ascribed to the blurring of chaotic motion by the additive noise.

Figure 12 shows new results from a simulation of the FHN system at high frequency in the suprathreshold regime. Panel A shows the interspike interval histogram for the noiseless suprathreshold case. The dynamics show 5:1 phase locking. Panel C shows the result when the amplitude is 0.06 instead of 0.04. There is an abrupt change to a 3:1 phase locking. Neither of these cases exhibits skipping. Panels B and D compare results for the same two amplitudes but with noise. One now sees the familiar skipping pattern, and further, there is a smoother transition from one pattern to the other as the amplitude (or noise, or both) changes. This combination of suprathreshold forcing with noise may thus underlie some of the skipping patterns seen experimentally.

We now turn to a model that best fits skipping data from electroreceptors. The goal of reporting this model here is again to show that “skipping” is not synonymous

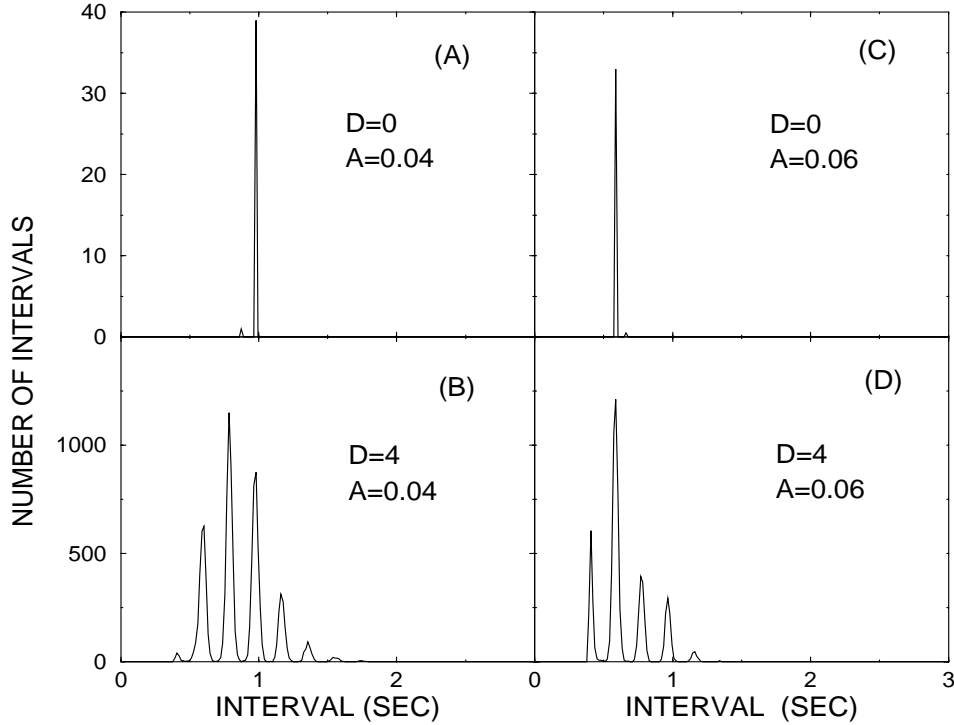
L198 *A. Longtin*


Fig. 12. Skipping in the suprathreshold regime of the FHN model Eq. (5). The forcing (angular) frequency is  $\omega_0 = 32$  ( $T = 0.196$ ). Noise intensities shown in legends must be multiplied by  $10^{-6}$ .

with “subthreshold”, and thus neither with “SR”. Also, by carefully modeling different statistics of the data, such as correlations between firing intervals, one may conclude very different roles for the noise. The model of interest is similar to the standard leaky integrate-and-fire model which has been analyzed in the SR context [37], except for an extra variable  $w$  governing the time dependence of the threshold. It is thus a two-variable model like the FHN model, but the transition to autonomous firing behavior is not of Hopf type. The model is:

$$dv/dt = -v/\tau_v + A[1 + \xi(t)] \sin(2\pi f_0 t) H[\sin(2\pi f_0 t)], \quad (6)$$

$$dw/dt = (w_0 - w)/\tau_w. \quad (7)$$

Here  $A$  is the amplitude of the forcing.  $H$  is the Heaviside function; it serves to truncate (or half-wave rectify) the sinusoidal signal. This is justified for many sensory neurons which respond to only one polarity of a physical stimulus (such as the opening of channels when hair cells are bent in one direction). A firing event occurs at the first instant in time (since the previous reset) when the voltage and threshold intersect. Physically, at such a crossing, the voltage exceeds threshold and a spike is generated. Assuming this occurs at time  $t$ , the voltage is reset to zero, i.e.  $v(t+) = 0$ , and the threshold is incremented by a fixed amount  $\Delta w$ , i.e.  $w(t+) = w(t) + \Delta w$ .

The recovery variable  $w$  appended here to the classic one-dimensional leaky integrate-and-fire model is similar to the  $w$  recovery variable used in the FHN system (thus its chosen name). We have chosen to model the dynamics using such a two-dimensional system instead of FHN because we have better control over the time scale of the memory effects following action potentials. Our efforts to obtain similar effects with FHN by modifying parameters such as  $\epsilon$  have been unsuccessful, which has led us to the leaky integrate-and-fire model with threshold dynamics (LIFDT). We do not have a proof that such memory effects are not possible with FHN, but we feel that what is probably needed is an extra variable. The FHN model is basically a relaxation oscillator with a fast time scale on the order of  $\epsilon$  and a slow one on the order of  $\epsilon^{-1}$ . We have not been able to modify the recovery time without significantly altering the shape of the action potentials. The advantage of using the LIFDT model is that the action potential itself is not represented; rather, only its effect is represented (voltage and threshold reset), allowing us to model the cumulative memory of firings a second variable. The linearity of the LIFDT model between firings also enables us to study many of its properties analytically, in contrast to FHN [45].

A realization of Eq. (7) is given in Fig. 13, along with the interval histogram. It is important to see that  $\Delta w$  is added to the value of the threshold at the time of firing, rather than to a fixed value. This has the effect of carrying the memory of previous firings over consecutive firing events. For example, if the cell has fired a few times in rapid succession, the threshold will have increased to a high value, with the result that the following firing will be delayed. Thus, long intervals are followed by short ones and vice versa, on average. This reproduces the experimentally observed negative correlation between intervals [38]. The model also produces skipping behavior over a wide range of parameters.

However, in order to get both the skipping behavior and the negative correlation between successive firing intervals, suprathreshold dynamics are needed according to our simulations. We could not find a parameter range where the model could exhibit both effects for subthreshold signals; the noise combined with the weakness of the signal tend to wash out the memory of preceding spikes. For suprathreshold dynamics, and in the absence of noise, this model simply produces 5:1 phase locking; the noise perturbs this phase locking pattern. P-type electroreceptors of weakly electric fish exhibit such histograms, and our analysis suggests a possible dynamical mechanism for this process. In particular, the model argues that skipping arises from noise, as opposed to subthreshold chaos as might occur in other systems [28]. This finding also motivates further theoretical studies of escape time distributions for suprathreshold stochastic dynamics.

Because the dynamics are suprathreshold, there is no enhancement of the periodic driving signal by increasing noise. However, noise can help code aperiodic signals in this suprathreshold regime. This occurs because the deterministic model exhibits phase locking, and noise can break up this phase locking. Over a range of amplitude  $A$  of the input, for example, the deterministic model produces a 5:1 phase locking pattern. The range is approximately given by the width of the Arnold tongue associated with 5:1 firing. If this input amplitude varies in time, mimicking the time variations of some stimulus, the model will not code these variations since it always gives a 5:1 pattern. However, if noise is added, the 5:1 pattern will be per-

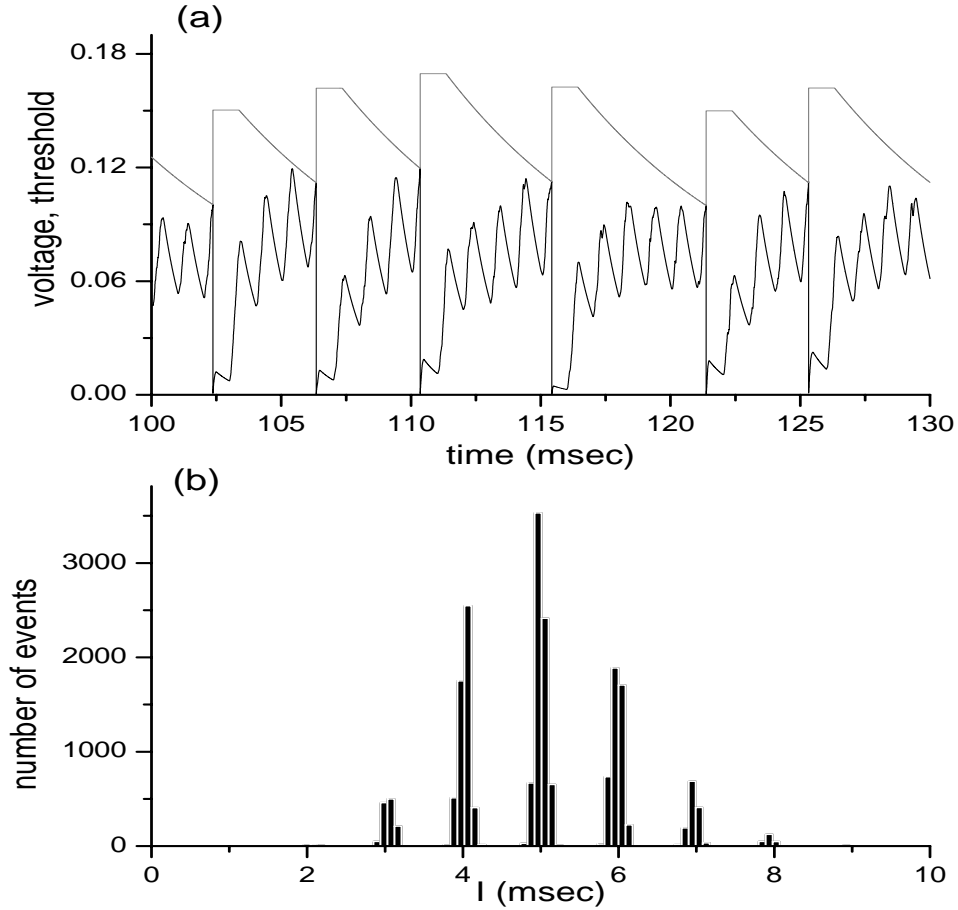
L200 *A. Longtin*

Fig. 13. Stochastic phase locking in the leaky integrate and fire model with threshold dynamics Eq. (7). Parameters are  $\tau_{uv} = 1$ ,  $\tau_w = 7.75$ ,  $A = 0.2613$ ,  $\Delta w = 0.05$ ,  $w_0 = 0.03$ ,  $f_0 = 1$  and  $D = 0.2063$ . A) Time series of the voltage from one realization, after transients have decayed. B) Interspike interval histogram.

turbed in a way that reflects the amplitude variations, and coding does occur [38]. Thus, noise can also help coding in the suprathreshold regime in certain cases.

## 8. Conclusion

We have summarized our analysis of stochastic phase locking in a variety of neural systems, and provided new results on the behavior of the SNR with noise and on suprathreshold dynamics. We have shown that the addition of noise to excitable dynamics brings a new perspective on issues of resonance and tuning. Noise linearizes the transduction function of the neuron, allowing its firing rate to track slow input signals. It also changes the shape of tuning curves, especially for mid-to-low forcing frequencies, i.e. frequencies below the preferred frequency of the neuron. For higher frequencies, i.e. in the non-adiabatic regime of the neuron subthreshold reso-

nances appear in the behavior of certain firing statistics [25,39]. There can be many such resonances, and while this is not clearly established, they appear associated with statistical versions of the deterministic suprathreshold phase-locked behaviors. Noise simply expresses these behaviors in the subthreshold regime. The precise connection between supra- and subthreshold resonances deserves more study. The study of those resonances will likely require analyses of the dynamics that account for the recovery variable behavior, such as the ones recently proposed in [10,32].

It is also of interest to see that SR studies have made their way into the fields of neurophysiology and bioengineering. SR is currently being investigated in medical applications such as sensory enhancement [9,40,41]. It has also been demonstrated in central (as opposed to “peripheral” or “sensory”) neurons with synaptic input [42]. We have performed analyses of SR without external forcing in bursting neurons, in which there exist, depending on the model, various internal oscillatory time scales [19,43]. Further, it has been recently shown that, with realistic parameters, correlations in Poisson inputs to a neuron have a similar effect to increasing noise [44]. This is because correlations between synaptic point processes increase the variance of the resulting input currents. Thus SR can be brought on by changing the number, activity and cross correlation of synaptic inputs.

Ultimately, the significance of SR will be established only when the neurons which receive output of neurons exhibiting SR actually care about the optimal statistic. It is certain however that, whether or not there are such postsynaptic neurons that do care, stochastic phase locking is a ubiquitous pattern used in neural coding, and that through our work and that of many others, we now have a better understanding for its genesis.

### Acknowledgements

The author gratefully acknowledges support from NSERC Canada and from CIHR Canada. The author also thanks Maurice Chacron for producing Fig. 13, as well as all his colleagues with whom he has discussed SR and stochastic phase locking over the last years.

### References

- [1] L. Glass and M. C. Mackey, *From Clocks to Chaos, The Rhythms of Life*, Princeton University Press, Princeton, N.J. (1988).
- [2] S. C. Müller, P. Coulet and D. Walgraef, Eds., *From Oscillations to Excitability — A Case Study in Spatially Extended Systems. Chaos* **4** (focus issue) (1994).
- [3] L. Gammaitoni, P. Hänggi, P. Jung and F. Marchesoni, *Stochastic resonance, Rev. Mod. Phys.* **70** (1998) 223–287.
- [4] T. Tateno, S. Doi, S. Sato and L. M. Ricciardi, *Stochastic phase lockings in a relaxation oscillator forced by a periodic input with additive noise — A first passage time approach, J. Stat. Phys.* **78** (1995) 917–935.
- [5] G. L. Gerstein and B. Mandelbrot, *Random walk models for the spike activity of a single neuron, Biophys. J.* **4** (1964) 41–68.
- [6] A. V. Holden, *Models of the stochastic activity of neurones*, Lect. Notes in Biomath. **12**, Springer Verlag, Berlin (1976).
- [7] H. Treutlein and K. Schulten, Ber. Bunsenges. *Phys. Chem.* **89** (1985) 710.

L202 A. Longtin

- [8] I. J. Hochmair-Desoyer, E. S. Hochmair, H. Motz and F. Rattay, *A model for the electrostimulation of the nervus acusticus*, *Neuroscience* **13** (1984) 553–562.
- [9] J. J. Collins, C. C. Chow and T. Imhoff, *Stochastic resonance without tuning*, *Nature* **376** (1995) 236–238.
- [10] A. Longtin, *Effect of noise on the tuning properties of excitable systems*, *Chaos, Solit. and Fract.* **11** (2000) 1835–1848.
- [11] B. Knight, *Dynamics of encoding in a population of neurons*, *J. gen. Physiol.* **59** (1972) 734–766.
- [12] L. Glass, C. Graves, G. A. Petrillo and M. C. Mackey, *Unstable dynamics of a periodically driven oscillator in the presence of noise*, *J. theor. Biol.* **86** (1980) 455–475.
- [13] Yu, X. and Lewis, E. R. *Studies with spike initiators: Linearization by noise allows continuous signal modulation in neural networks*, *IEEE Trans. Biomed. Eng.* **36** (1989) 36–43.
- [14] J. P. Segundo, J. F. Vibert, K. Pakdaman, M. Stiber and O. D. Martinez, in *Origins: Brain and Self Organization*, K. Pribram, ed. (1994)
- [15] A. Pikovsky and J. Kurths, *Coherence resonance*, *Phys. Rev. Lett.* **78** (1997) 775–778.
- [16] B. Shulgin *et al.*, *Phys. Rev. Lett.* **75** (1995) 4157–4160.
- [17] A. Neiman, A. Silchenko, V. Anishchenko and L. Schimansky-Geier, *Stochastic resonance: noise enhanced phase coherence*, *Phys. Rev. E.* (1999).
- [18] Tuckwell, H. C. *Stochastic Processes in the Neurosciences*, CBMS-NSF Regional Conference Series in Applied Mathematics Vol. **56**. Soc. for Industrial and Applied Mathematics, Philadelphia (1989).
- [19] A. Longtin and K. Hinzer, *Encoding with bursting, subthreshold oscillations and noise in mammalian cold receptors*, *Neural Comput.* **8** (1996) 215–255.
- [20] J. K. Douglass, L. Wilkens, E. Pantazelou and F. Moss, *Noise enhancement of information transfer in crayfish mechanoreceptors by stochastic resonance*, *Nature* **365** (1993) 337–340.
- [21] B. Lindner and L. Schimansky-Geier, *Transmission of noise coded versus additive signals through a neuronal ensemble*, *Phys. Rev. Lett.* **86** (2001) 2934–2937.
- [22] P. Lánský and L. Sacerdote, *The Ornstein-Uhlenbeck neuronal model with signal-dependent noise*, *Phys. Lett. A* **285** (2001) 132–140.
- [23] K. Wiesenfeld *et al.*, *Stochastic resonance on a circle*, *Phys. Rev. Lett.* **72** (1994) 2125–2128.
- [24] A. Longtin, *Stochastic resonance in neuron models*, *J. Stat. Phys.* **70** (1993) 309.
- [25] A. Longtin and D. R. Chialvo, *Stochastic and deterministic resonances in excitable systems*, *Phys. Rev. Lett.* **81** (1998) 4012–4015.
- [26] D. R. Chialvo, A. Longtin and J. Muller-Gerking, *Stochastic resonance in models of neuronal ensembles*, *Phys. Rev. E* **55** (1997) 1798–1808.
- [27] J. K. Douglass, F. Moss and A. Longtin, *Statistical and dynamical interpretation of ISIH data from periodically stimulated sensory neurons*. Proceedings, *Fifth Neural Information Processing Systems (NIPS) Conference*, S. J. Hanson, J. Cowan and L. Giles, eds. (Morgan-Kaufmann, Mateo, CA, 1993) 993–1000.
- [28] D. T. Kaplan, J. R. Clay, T. Manning, L. Glass, M. R. Guevara and A. Shrier, *Phys. Rev. Lett* **76** (1996) 4074–4077.
- [29] J. J. Collins, C. C. Chow and T. Imhoff, *Aperiodic stochastic resonance*, *Phys. Rev. E* **52** (1995) 3321–3324.
- [30] J. E. Levin and J. P. Miller, *Broadband neural encoding in the cricket cercal sensory system enhanced by stochastic resonance*, *Nature* **380** (1996) 165–168.

- [31] A. Longtin and M. St-Hilaire, *Encoding carrier amplitude modulations via stochastic phase synchronization*, *Int. J. Bifurc. Chaos* **10** (2000) 1–16.
- [32] B. Lindner and L. Schimansky-Geier, *Phys. Rev. E* (2000).
- [33] A. Longtin, A. Bulsara and F. Moss, *Time interval sequences in bistable systems and the noise induced transmission of information by sensory neurons*, *Phys. Rev. Lett.* **67** (1991) 656–659.
- [34] Z. Gingl, L. B. Kiss and F. Moss, *Non-dynamical stochastic resonance: Theory and experiments with white and various coloured noises*, *Nuovo Cimento D* **17** (1995) 795–802.
- [35] P. Jung, *Threshold devices: fractal noise and neural talk*, *Phys. Rev. E* **50** (1994) 2513–2522.
- [36] P. Jung and P. Hänggi, *Phys. Rev. A* **44** (1991) 8032.
- [37] T. Shimokawa, K. Pakdaman and S. Sato, *Time scale matching in the response of a leaky integrate-and-fire neuron model to periodic stimulus with additive noise*, *Phys. Rev. E* **59** (1999) 3427–3443.
- [38] M. Chacron, A. Longtin, M. St-Hilaire and L. Maler, *Suprathreshold stochastic firing dynamics with memory in P-type electroreceptors*, *Phys. Rev. Lett.* **85** (2000) 1576–1579.
- [39] S. Ripoll Massanés and C. J. Pérez Vicente, *Nonadiabatic resonances in a noisy FitzHugh-Nagumo neuron model*, *Phys. Rev. E* **59** (1999) 4490–4497.
- [40] P. J. Cordo, J. T. Inglis, J. J. Collins, S. M. P. Verschueren, D. M. Merfeld, S. Buckley and F. Moss, *Noise-enhanced information transmission in human muscle spindles via stochastic resonance*, *Nature* **383** (1996) 769–770.
- [41] R. P. Morse and E. F. Evans, *Enhancement of vowel coding for cochlear implants by addition of noise*, *Nature Med.* **2** (1996) 928–932.
- [42] W. C. Stacey and D. M. Durand, *Synaptic noise improves detection of subthreshold signals in hippocampal CA1 neurons*, *J. Neurophysiol.* **86** (2001) 1104–1112.
- [43] A. Longtin, *Autonomous stochastic resonance in bursting neurons*, *Phys. Rev. E* **55** (1997) 868–876.
- [44] M. Rudolph and A. Destexhe, *Correlation detection and resonance in neural systems with distributed noise sources*, *Phys. Rev. Lett.* **86** (2001) 3662–3665.
- [45] M. J. Chacron, K. Pakdaman and A. Longtin, *Interspike interval correlations, memory, adaptation and refractoriness in a leaky integrate-and-fire model with threshold fatigue*, *Neural Comput.* **15** (in press, 2002).